

Jump frequencies of Cd tracer atoms in L₁₂ lanthanide gallides

Xia Jiang^{1, a}, Matthew O. Zacate^{2, b} and Gary S. Collins^{1, c}

¹Dept. of Physics and Astronomy, Washington State University, Pullman, WA, USA

²Dept. of Physics and Geology, Northern Kentucky University, Highland Heights, KY, USA

^ajiangsxia@uchicago.com, ^bzacatem1@nku.edu, ^ccollins@wsu.edu

Keywords: Diffusion, jump frequency, perturbed angular correlation, PAC, nuclear hyperfine interaction, nuclear relaxation, intermetallic compounds, L₁₂ structure.

Abstract. Jump frequencies of Cd tracer atoms were measured in three lanthanide gallides having the L₁₂ structure: DyGa₃, ErGa₃ and LuGa₃. ¹¹¹In/Cd impurity probe atoms were observed to occupy the non-cubic Ga-sites through the nuclear quadrupole interaction using the method of perturbed angular correlation of gamma rays (PAC). Measurements at elevated temperatures exhibited nuclear relaxation (damping) of quadrupolar perturbation functions attributed to diffusional jumps of the probes among orientationally inequivalent Ga-sites. Accurate values of jump frequencies were determined from fits of the measured perturbation functions using a model of stochastically fluctuating electric-field gradients, as in previous work [e.g., Matthew O. Zacate, Aurélie Favrot and Gary S. Collins: Physical Review Letters Vol. 92 (2004) p. 225901]. Arrhenius plots of jump frequencies for the three systems exhibited jump-frequency activation enthalpies in the range 0.86-1.05 eV and prefactors of about 2 THz. The activation enthalpy for ErGa₃, 0.86(2) eV is compared with those for ErAl₃, 1.40(4) eV, and ErIn₃, 1.34(5) eV.

Introduction

Methods for detecting atom movement in solids can be broadly classified as macroscopic or microscopic [1,2]. The classic macroscopic method is depth profiling of tracer atoms by sectioning [3]. Among microscopic methods, the most direct are those that measure jump-frequencies of tracer probe atoms. For diffusion on sublattices in cubic systems, the diffusivity D is proportional to the jump-frequency w (inverse of the mean residence time) through the relation

$$D = \frac{1}{6} f \ell^2 w, \quad (1)$$

in which ℓ is the jump distance and f is the correlation factor. One approach to detect jump frequencies is through measurement of nuclear relaxation caused by stochastic changes in the environments of a set of probe nuclei. Such a method is familiar from nuclear resonance [2] and Mössbauer effect [2] studies.

Recently, two of us showed that jump frequencies could also be measured using the technique of perturbed angular correlation of gamma rays (PAC) [4]. Stochastic changes in the magnitude or orientation of the electric field gradient (EFG) at probe nuclei during the lifetime of the PAC level lead to decoherence of precessions of the nuclear quadrupole moments. This was demonstrated for ¹¹¹In/Cd probe atoms in rare-earth indides of nominal composition A₃B having the L₁₂ structure [4,5,6] and also in several stannides [6,7]. As can be seen from Fig. 1, the A-sublattice has three orientationally inequivalent sites, with tetragonal axes along X, Y and Z cube directions. The tetragonal axes are local principal axes of the electric-field gradient tensors about which, figuratively, the quadrupole moments precess. Each jump of an atom on the A-sublattice caused, for example, by rapid passage of a lattice vacancy diffusing on the A-sublattice, leads to reorientation of the local tetragonal axis of symmetry by 90° and to decoherence in the nuclear precessions.

All measurements in present and past reported work were made using the $^{111}\text{In}/\text{Cd}$ probe. ^{111}In decays with a mean life of 4.0 days into the second excited state of ^{111}Cd , followed by successive emission of two gamma rays having energies of 173 and 245 keV. The intermediate, or PAC level, at 245 keV, has a long mean life, 120 ns, and spin 5/2. There is an angular anisotropy in the direction of emission of the second gamma ray relative to the first. A PAC spectrometer consists of pairs of gamma ray detectors set up at fixed angles relative to the source to measure lifetime distributions of the intermediate level. The anisotropy and nuclear precessions caused by hyperfine interactions result in alternatingly greater and less than average coincidence counting rates. Accumulated delayed coincidence lifetime curves are fitted to obtain the PAC perturbation function, which contains all information about the extranuclear environment(s) of the probe nuclei. For spin 5/2 and a random distribution of interaction orientations, the static quadrupole perturbation function is given by

$$G_2^{static}(t) = \frac{1}{5} \left\{ 1 + \frac{13}{7} \cos(6\omega_Q t) + \frac{10}{7} \cos(12\omega_Q t) + \frac{5}{7} \cos(18\omega_Q t) \right\}, \quad (2)$$

in which $\omega_Q = \frac{\pi}{20} eQV_{zz} / h$ is the quadrupole interaction frequency between the quadrupole moment Q and electric field gradient V_{zz} , and e and h are the electronic charge and Planck's constant. Eq. 2 applies when there is at least a three-fold axis of charge symmetry through the nuclear site, as there is for the tetragonal A-site. For the B-site, which has cubic point symmetry, $V_{zz} = 0$. Further information about PAC spectroscopy and methods can be found in refs. [8] and [9].

Diffusion by jumps on the A-sublattice is a realization of the so-called XYZ relaxation model, in which the EFG axis fluctuates stochastically among the three cube directions. Analysis by Baudry and Boyer [10] showed that, to a good approximation, the dynamically relaxed perturbation function $G_2(t)$ is given in terms of the static function $G_2^{static}(t)$ by

$$G_2(t) = \exp(-wt) \cdot G_2^{static}(t), \quad (3)$$

in which the relaxation frequency is equal to the jump frequency w (inverse of the mean residence time). (It should be noted that w was defined differently in ref. [10], as the rate at which the EFG fluctuates from one direction to a single other direction, so that our definition is twice larger.) Eq. 3 applies in the so-called slow fluctuation regime, when $w < \omega_Q$. It has been shown that analysis using the Baudry and Boyer approximation underestimates jump frequencies slightly at higher temperatures [11], so that fitted activation enthalpies would be largely correct but frequency prefactors would be underestimated. To get the most reliable values, spectra were fitted in the present work with exact numerical calculations for the XYZ model, as in ref. [4,5,6].

The present work is a study of jump frequencies of Cd probe atoms in rare-earth gallides having the $L1_2$ structure, carried out for comparison with previous studies on indides and stannides. The phases studied were DyGa_3 , ErGa_3 and LuGa_3 . ErAl_3 was also studied. In the indides previously studied, ^{111}In probe atoms were host atom constituents. Although the indide phases (and present

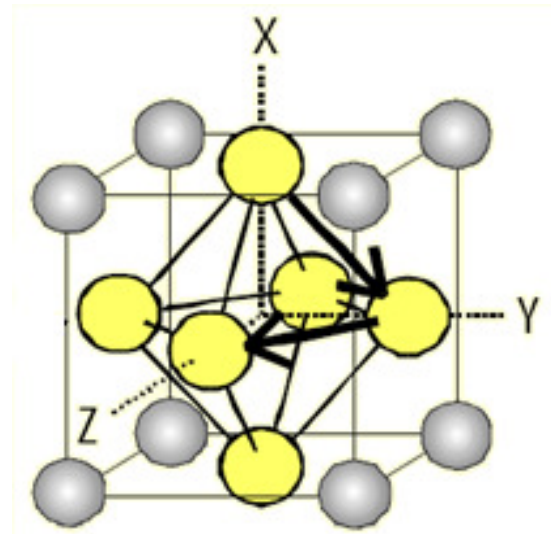


Fig. 1. $L1_2$ crystal structure of A_3B phase. Each jump on the A-sublattice leads to reorientation of the axis of the EFG tensor among the X, Y and Z directions.

gallium phases) appear as line compounds in binary phase diagrams, of necessity there must be a small, non-zero width to the $L1_2$ phase field. Previous measurements on indide phases LaIn_3 and CeIn_3 were carried out using pairs of samples that had been prepared so as to have an excess or deficit of indium [4,5]. It was found that jump frequencies were 10-100 times greater at the A-rich phase boundary than at the A-poorer boundary in A_3B . Possible reasons for this were discussed in [4] and are the subject of a more extensive study on indide phases in progress.

Similar studies were made of jump frequencies of $^{111}\text{In}/\text{Cd}$ probes in two stannides, LaSn_3 [6] and CeSn_3 [7]. There, the probe was an impurity and might preferentially occupy either the tetragonal A-site or cubic B-site. In practice, it had a strong preference to occupy the A- or Sn-site.

Sample preparation and measurements

Rare-earth and gallium metals of 99.9% and 99.9999% purity, respectively, were melted with carrier-free ^{111}In activity in a small arc-furnace after purging the furnace with argon to prevent oxidation. The ^{111}In activity was highly dilute, with a mole fraction of about 10^{-8} . Resulting sources were spherical, indicating good mixing in the liquid state, and had masses of about 80 mg. X-ray measurements confirmed that the dominant phase was $L1_2$. Appreciable mass losses occurred during melting and were used in conjunction with the nominal composition to define upper and lower limits of the actual compositions. Measurements were made using a four-counter PAC spectrometer and oven described previously [12]. Measurements were also made on ErAl_3 in order to compare jump frequencies of Cd tracers in the series ErIn_3 [5], ErGa_3 and ErAl_3 .

Initial measurements were made on ErGa_3 samples with boundary compositions that were Ga-richer and Ga-poorer. Nominal compositions were about 22 at.% and 28 at.% Er, so that the samples consisted mostly of ErGa_3 at the A-rich phase boundary composition (designated A) and the A-poorer boundary composition (designated B), with minor amounts of neighboring phases: Ga-metal for boundary A, and Ga_2R for boundary B. Representative PAC spectra are shown in Fig. 2 as a function of the time delay between emission of the first and second gamma rays. The data at apparently negative time is completely equivalent to data measured at positive time and shows relaxation more clearly below. The A-rich spectrum (Fig. 2a) is dominated by a large positive offset that is attributed to probe atoms on the cubic Er-site. The A-poorer spectrum (Fig. 2b) is dominated by a precessional signal attributed to probe atoms on Ga-sites. Each spectrum exhibits a minor site fraction due to probe atoms on the other sublattice. The observed site fractions in Fig. 2 are consistent with the heuristic rule that impurities tend to occupy the sublattice of an element in which there is a deficiency [9]. The much lower site-fraction and poorer statistical quality for probes on the Ga-sublattice in A-rich samples led us to analyze nuclear relaxation only in Ga-poorer samples (at boundary composition B).

All spectra exhibited excellent signal homogeneity at low temperatures, indicating the presence of only very small

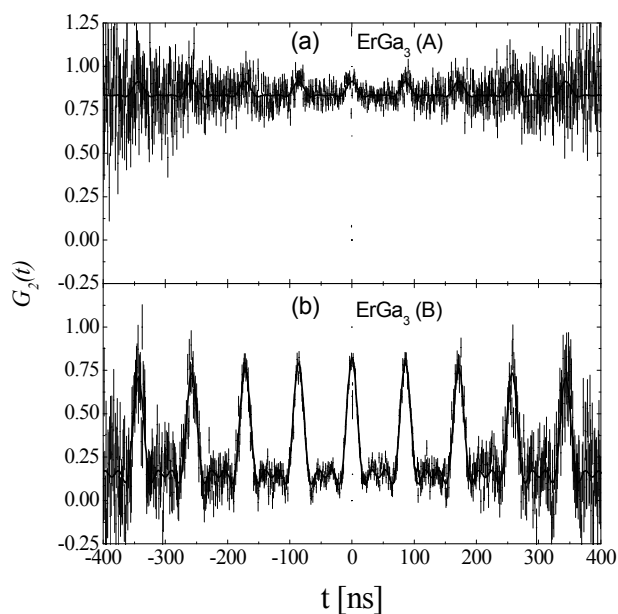


Fig. 2. PAC spectra of In/Cd impurity probe atoms in samples of ErGa_3 that were Ga-rich (a) or Ga-poor (b).

EFGs caused by lattice disorder. Good signal homogeneity also indicates that the compositions at phase boundaries B were very close to the stoichiometric composition (probably closer than about 0.1-0.2 at.% [4]).

Results

Spectra measured at boundary composition B were dominated by a single, axially symmetric quadrupole perturbation function having interaction frequencies ω_Q in DyGa₃, ErGa₃ and LuGa₃ measured to be 10.78(1), 12.36(1) and 12.08(1) Mrad/s, respectively, at 673 K. The frequency for ErAl₃ at 804 K was 12.39(2) Mrad/s. These values are similar to those observed in corresponding lanthanide indide phases [6]. Measurements were made at temperatures up to 1130 K. Fig. 3 shows PAC spectra for ErGa₃ measured at the four indicated temperatures. Spectra for the three lower temperatures exhibit damped oscillations as described by eq. 3. The spectrum at the highest temperature is in the fast fluctuation regime, with $w > \omega_Q$ [4, 5] and is not described by eq. 3.

An Arrhenius plot of the jump frequencies obtained by fitting spectra with numerical calculations of the XYZ model is shown in Fig. 4. The five data sets are described well by thermally activated expressions of the form

$$w = w_0 \exp(-Q/k_B T), \quad (4)$$

in which Q and w_0 are the jump-frequency activation enthalpy and prefactor. Jump frequencies below 1 MHz can not be fitted as precisely due to finite lifetime of the PAC nuclear level. Especially for DyGa₃ and LuGa₃, fitted frequencies at lower temperatures appear to be enhanced. This might be due to small amounts of inhomogeneous broadening or to another diffusion mechanism becoming significant in the lower temperature range, but the cause was not resolved in this study.

Lines drawn in Fig. 4 are results of fitting the 5-7 points at highest temperatures using Eq. 4, with fitted results given in Table 1. Also included in the table are results for ErIn₃ from another study [13] and lattice parameters [14]. All measurements are at the B-richer boundary compositions (B), including the one for ErIn₃.

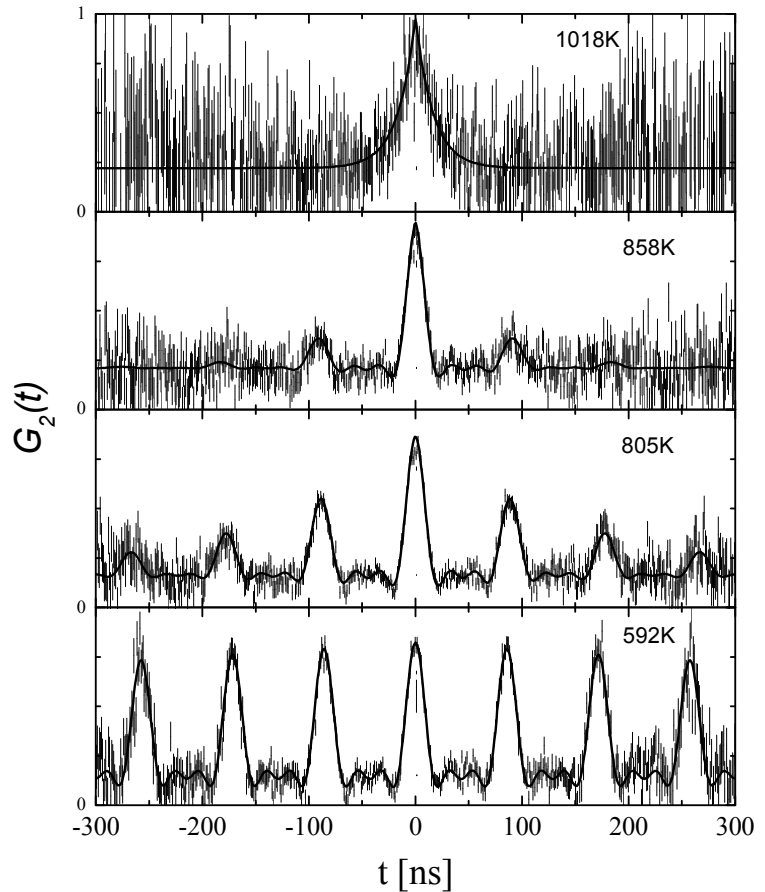


Fig. 3. PAC spectra in ErGa₃ measured at the indicated temperatures. With increasing temperature, greater nuclear relaxation is observed that is attributed to diffusional jumps of Cd-probe atoms on the Ga-sublattice.

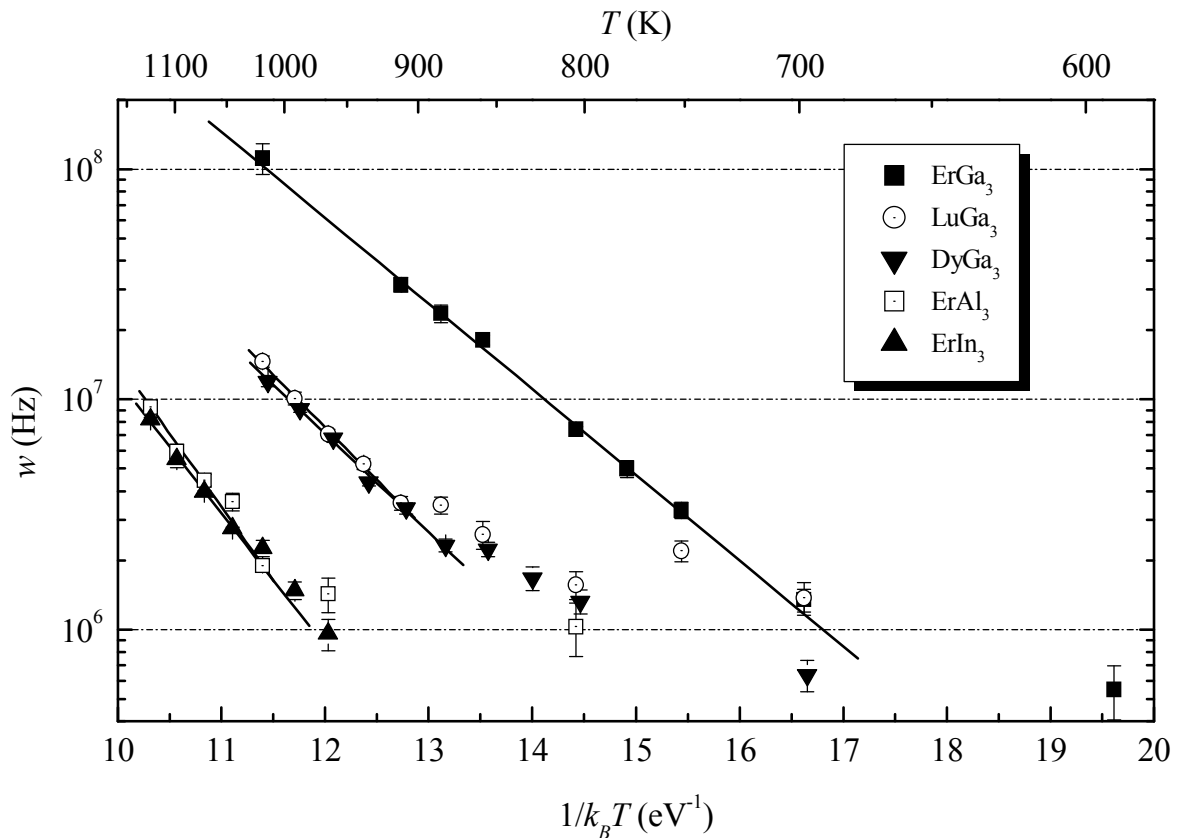


Fig. 4. Arrhenius plots of jump frequencies of Cd-probe atoms on Ga-, Al- and In-sublattices in the indicated phases.

Table 1. Activation enthalpies and jump frequency prefactors for Cd tracers jumping on the A-sublattices in A_3B phases (A= Ga,Al,In).

Phase	Q (eV)	w_0 (THz)	a (Å)	Source of data
DyGa ₃	0.98(4)	$0.95^{+0.53}_{-0.34}$	4.271	This work
LuGa ₃	1.05(3)	$2.2^{+1.1}_{-0.7}$	4.180	This work
ErGa ₃	0.86(2)	$1.8^{+0.8}_{-0.5}$	4.206	This work
ErAl ₃	1.40(4)	16^{+9}_{-6}	4.215	This work
ErIn ₃	1.34(5)	$7.7^{+5.7}_{-3.2}$	4.564	[13]

Discussion

As can be seen from Fig. 1, each site on the A-sublattice has 8 A-atoms and 4 B-atoms near neighbors. The A-sublattice spans the crystal and the simplest diffusion mechanism for atoms on the A-sublattice is sublattice vacancy diffusion, in which an A-vacancy and atom exchange places. In a simple version of this mechanism, the jump frequency for an impurity atom can be expressed as

$$w = 8[V_A] \exp(+E_B / k_B T) w_2, \quad (5)$$

in which $[V_A]$ is the mole fraction of vacancies on the A-sublattice, E_B is the binding enthalpy between the Cd impurity and an A-vacancy, and w_2 is the exchange frequency between the Cd impurity and a neighboring vacancy. It must be noted that no signal has ever been observed in past or present measurements on indides, gallides or the aluminide that could be attributed to a nearby defect such as a vacancy. If such a defect resided for a significant time next to the impurity probe

atom, it would produce a disturbing EFG having a differing magnitude and lower symmetry, leading to a perturbation function distinct from that of a defect-free tracer given in Eq. 2. Consequently, it is assumed that any such vacancy defects pass rapidly through the local vicinity of the probe atom, while shuffling tracer atoms and other A-sublattice atoms to neighboring sites with different EFG orientations. The exchange frequency will be assumed to be thermally activated with a frequency prefactor w_{20} of the order of the vibrational frequency of an atom about its mean position subject to an enthalpy barrier for migration E_M : $w_2 = w_{20} \exp(-E_M / k_B T)$

The general aspect of binary phase diagrams for these A-B alloys is that A_3B systems have neighboring phases that are pure A-metal on the A-rich side and a more B-rich intermediate phase such as A_2B or A_5B_3 on the B-rich site. We note that melting temperatures of the A_3B and more B-rich phases are comparable and much greater than for the pure-A metal phase. The large differences in melting temperatures suggest that composition dependences of free energy curves for the three phases at a given temperature have much deeper minima for the two intermediate phases than for the terminal metal phase. Since boundary compositions are determined from tangent constructions underlying free energy curves [15], the A-poor phase boundary compositions of our samples are likely to be very close to the stoichiometric composition. Consequently, there must be very few structural point defects and, as a consequence, any A-vacancies necessary for diffusion must be thermally activated. Such thermal activation involves formation of combinations of elementary defects that preserve the overall composition of the alloy (for the $L1_2$ structure, see, e.g., see [16]). However, in the following we shall assume a simplified model in which the vacancy mole fraction $[V_A]$ is assumed to be thermally activated with an effective mole-fraction prefactor c_0 and formation enthalpy E_F^{eff} , $[V_A] = c_0 \exp(-E_F^{eff} / k_B T)$, so that eq. 5 can be written as

$$w = 8c_0 w_{20} \exp(-(E_F^{eff} + E_M - E_B) / k_B T). \quad (6)$$

We use eq. 6 to interpret the experimental results given in Table 1. According to the above model, the experimental jump-frequency activation enthalpy is equal to $Q = E_F^{eff} + E_M - E_B$ and the jump-frequency prefactor to $w_0 = 8c_0 w_{20}$. Since no defects such as for vacancies have been detected next to the impurity In/Cd tracers, we assume that the binding enthalpy E_B in these systems is small and probably close to zero, say within ± 0.1 eV. Since 2/3 of the atoms neighboring an A-vacancy are A-atoms, it is reasonable to suppose that the effective formation enthalpy will be close to the vacancy formation enthalpy in the pure A-metal host. These have been measured by positron annihilation to be 0.68(3) and 0.55(2) eV, respectively, for aluminum and indium metals [17], and by a combination of lattice parameter and length change measurements to be 0.23 eV for gallium metal [18]. For $ErAl_3$, with $Q = 1.40$ eV, from eq. 6 one obtains $E_M \approx 0.7$ eV, which is in reasonable agreement with $E_M \approx 0.6$ eV determined from a study of annealing of excess vacancies by Mössbauer spectroscopy [19]. For $ErIn_3$, with $Q = 1.34$ eV, one obtains in the same way $E_M \approx 0.8$ eV, although no value is known for comparison. Finally, for the gallides, $Q \sim 0.95$ eV yields $E_M \approx 0.7$ eV, for which we also have no value for comparison. These appear to be reasonable values, and it is noteworthy that jump-frequency activation enthalpies Q are correlated with vacancy formation enthalpies of the pure-A host metals given above. Fitted jump-frequency prefactors are all in the range 1-15 THz, approximately equal to the vibrational frequency of an atom in a solid, which is taken to support the assumed sublattice vacancy diffusion mechanism.

Comparison with other methods

Since the PAC method for measuring jump frequencies is not well known, we point out favorable features and limitations of the method. Favorable features are:

- (1) A data point such as in Fig. 4 can be measured typically in one day, with up to ~10 measurements possible using a single sample.
- (2) For “line compounds” such as studied here, having very narrow phase fields, measurements can be conveniently and accurately made at each of the opposing boundary compositions. This is because the presence of small volume fractions of other phases does not interfere with a PAC measurement since quadrupole interactions of signals from neighboring phases can generally be resolved. By contrast, measurements of the diffusivity at phase boundary compositions are uncertain due to ambiguities connected with diffusion in multi-phase systems (e.g., rapid diffusion along grain boundaries between phases.)
- (3) Previous PAC measurements [4] in line compounds demonstrated differences in jump frequencies at opposing boundary compositions by ratios up to 1000, indicating the crucial role of composition in determining diffusivities in nominal line compounds [20]. These ratios are easily measured using the PAC method.

Limitations of the method are:

- (1) The method requires that diffusional jumps lead to changes in magnitude or orientation of the local EFG. Thus, it will not work for tracers on cubic sites or when jumps do not lead to changes in the EFG, such as, for example, diffusion in a noncubic metal such as Zn.
- (2) Only a limited number of probes having favorable nuclear parameters are available for measurements. The common probes for “table top” experiments are $^{111}\text{In}/\text{Cd}$ and $^{181}\text{Hf}/\text{Ta}$. A small number of more exotic probes are available using online facilities such as ISOLDE at CERN that can produce and implant PAC isotopes having short-lived parent states [21].
- (3) For impurity tracers, one has to check experimentally that the tracer actually occupies the desired site. As we have found in past studies, site preferences of impurities can not be simply assumed on the basis of naïve notions of impurity chemistry or atom size.

Summary

Nuclear relaxation of quadrupole interactions of Cd tracer atoms was measured in four gallide and aluminide A_3B phases having the L1_2 structure using PAC. These so-called “line compounds” had A-poor boundary compositions that were argued to be very close to the stoichiometric compositions. The relaxation was attributed to diffusional jumps on the A-sublattice, leading to reorientation of axes of the EFG by 90 degrees in each jump, as observed in previous studies on indides having the same structure. Measured jump-frequency activation enthalpies and prefactors showed that the observations are broadly consistent with a sublattice vacancy diffusion mechanism. Using a simplified model, jump-frequency activation enthalpies are shown to be correlated with the formation enthalpy of vacancies in the pure-A host metals, and jump-frequency prefactors are found to be of the order of 1-10 THz, the vibrational frequency of an atom in a solid.

Acknowledgments

This research was supported in part by the National Science Foundation under grants DMR 05-04843 (Metals Program) at Washington State University and DMR 06-06006 (Metals Program) at Northern Kentucky University. Computational facilities were provided in part by Kentucky EPSCOR grant RSF 012-03.

References

-
- [1] Helmut Mehrer, *Diffusion in Solids* (Springer, Germany 2007).
- [2] Jörg Kärger, Paul Heitjans and Reinhold Haberlandt, eds.: *Diffusion in Condensed Matter* (Vieweg, Braunschweig 1998).
- [3] H. Mehrer: *Diffusion in Solid Metals and Alloys*, edited by H. Mehrer, Landolt-Börnstein NS III, Vol. 26 (Springer, Berlin, 1990), p. 1.
- [4] Matthew O. Zacate, Aurélie Favrot and Gary S. Collins: *Physical Review Letters* Vol. 92 (2004) 225901; and Erratum, *Physical Review Letters* 93 (2004) p. 049903
- [5] G.S. Collins, A. Favrot, L. Kang, D. Solodovnikov and M.O. Zacate: *Defect and Diffusion Forum* Vol. 237-240 (2005) p. 195-200
- [6] Gary S. Collins, Aurélie Favrot, Li Kang, Egbert Rein Nieuwenhuis, Denys Solodovnikov, Jipeng Wang and Matthew O. Zacate: *Hyperfine Interactions* 159 (2004) p. 1-8
- [7] Benjamin Norman: unpublished (2007).
- [8] Günter Schatz and Alois Weidinger: *Nuclear Condensed-Matter Physics* (Wiley, New York, 1996).
- [9] Matthew O. Zacate and Gary S. Collins: *Physical Review B* Vol. 70 (2004) p. 24202
- [10] A. Baudry and P. Boyer: *Hyperfine Interactions* Vol. 35 (1987) p. 803
- [11] Matthew O. Zacate and William E. Evenson: *Hyperfine Interactions* Vol. 158 (2004) p. 329-332
- [12] Matthew O. Zacate and Gary S. Collins: *Physical Review B* Vol. 69 (2004) p. 174202
- [13] Xia Jiang et al.: (to be published).
- [14] *Binary Alloy Phase Diagrams*, edited by T.B. Massalski (ASM International, second ed., 1990).
- [15] See, e.g., A. Prince: *Alloy phase equilibria* (Elsevier, Amsterdam 1966).
- [16] Gary S. Collins and Matthew O. Zacate: *Hyperfine Interactions* Vol. 136/137 (2001) p. 641-646
- [17] H.-E. Schaeffer: *Physica Status Solidi (a)* Vol. 102 (1987) p. 47-65
- [18] G. Mair, K. Hamacher and H. Wenzl: *Zeitschrift fuer Physik B* Vol. 24 (1976) p. 301-5
- [19] K. Sassa, W. Petry and G. Vogl: *Philosophical Magazine A* Vol. 48 (1983) p. 41
- [20] Gary S. Collins: *Journal of Materials Science* Vol. 42 (2007) p. 1915-1919
- [21] See, e.g., J.G. Correia: *Nuclear Instruments and Methods in Physics Research B* Vol. 136-8 (1998) p. 736 -743

Diffusion in Materials

doi:10.4028/www.scientific.net/DDF.289-292

Jump Frequencies of Cd Tracer Atoms in L1₂ Lanthanide Gallides

doi:10.4028/www.scientific.net/DDF.289-292.725

References

- [1] Helmut Mehrer, Diffusion in Solids (Springer, Germany 2007).
- [2] Jörg Kärgel, Paul Heitjans and Reinhold Haberlandt, eds.: Diffusion in Condensed Matter (Vieweg, Braunschweig 1998).
- [3] H. Mehrer: Diffusion in Solid Metals and Alloys, edited by H. Mehrer, Landolt-Börnstein NS III, Vol. 26 (Springer, Berlin, 1990), p. 1.
doi:10.1007/10390457_1
- [4] Matthew O. Zacate, Aurélie Favrot and Gary S. Collins: Physical Review Letters Vol. 92 (2004) 225901; and Erratum, Physical Review Letters 93 (2004) p. 049903
- [5] G.S. Collins, A. Favrot, L. Kang, D. Solodovnikov and M.O. Zacate: Defect and Diffusion Forum Vol. 237-240 (2005) p. 195-200
doi:10.4028/www.scientific.net/DDF.237-240.195
- [6] Gary S. Collins, Aurélie Favrot, Li Kang, Egbert Rein Nieuwenhuis, Denys Solodovnikov, Jipeng Wang and Matthew O. Zacate: Hyperfine Interactions 159 (2004) p. 1-8
doi:10.1007/s10751-005-9073-8
- [7] Benjamin Norman: unpublished (2007).
- [8] Günter Schatz and Alois Weidinger: Nuclear Condensed-Matter Physics (Wiley, New York, 1996).
- [9] Matthew O. Zacate and Gary S. Collins: Physical Review B Vol. 70 (2004) p. 24202
doi:10.1103/PhysRevB.70.024202
- [10] A. Baudry and P. Boyer: Hyperfine Interactions Vol. 35 (1987) p. 803
doi:10.1007/BF02394496
- [11] Matthew O. Zacate and William E. Evenson: Hyperfine Interactions Vol. 158 (2004) p. 329-332
doi:10.1007/s10751-005-9049-8
- [12] Matthew O. Zacate and Gary S. Collins: Physical Review B Vol. 69 (2004) p. 174202
doi:10.1103/PhysRevB.69.174202

[13] Xia Jiang et al.: (to be published).

[14] Binary Alloy Phase Diagrams, edited by T.B. Massalski (ASM International, second ed., 1990).

[15] See, e.g., A. Prince: Alloy phase equilibria (Elsevier, Amsterdam 1966).

[16] Gary S. Collins and Matthew O. Zacate: Hyperfine Interactions Vol. 136/137 (2001) p. 641-646

doi:10.1023/A:1020538925066

[17] H.-E. Schaeffer: Physica Status Solidi (a) Vol. 102 (1987) p. 47-65

doi:10.1002/pssa.2211020104

[18] G. Mair, K. Hamacher and H. Wenzl: Zeitschrift Fuer Physik B Vol. 24 (1976) p. 301-5

[19] K. Sassa, W. Petry and G. Vogl: Philosophical Magazine A Vol. 48 (1983) p. 41

doi:10.1080/01418618308234886

[20] Gary S. Collins: Journal of Materials Science Vol. 42 (2007) p. 1915-1919

doi:10.1007/s10853-006-0055-2

[21] See, e.g., J.G. Correia: Nuclear Instruments and Methods in Physics Research B Vol. 136-8 (1998) p. 736 -743